Invariant Spatial Parametrization of Human Thoracohumeral Kinematics: A Feasibility Study *

Rakesh Krishnan[1,2], Niclas Björsell[2] and Christian Smith[1]

***Abstract*—In this paper, we present a novel kinematic framework using hybrid twists, that has the potential to improve the reliability of estimated human shoulder kinematics. This is important as the functional aspects of the human shoulder are evaluated using the information embedded in thoracohumeral kinematics. We successfully demonstrate in our results, that our approach is invariant of the body-fixed coordinate definition, is singularity free and has high repeatability; thus resulting in a flexible user-specific kinematic tracking not restricted to bony landmarks.**

I. Introduction

In the past decade, robot-assisted therapy and rehabilitation interventions for human upper limb have gained momentum leading to many exoskeleton-based solutions. These upper limb exoskeletons are required to work closely with the human anatomic joints. Hence, it is important to ensure user's safety and comfort [1]. Robust and reliable sensing of human upper limb kinematics is essential, not only for operation of these devices, but also in their functional evaluation.

Human joints are structurally and functionally different compared to anthropomorphic robots. A major bottleneck for reliable kinematic tracking, is the lack of consensus among researchers on suitable mathematical representations [2], to parametrise human shoulder kinematics. For such applications, that aim at functional compensation through human-machine interaction, some experts suggest that the computational reliability requirement should not be less than 100% [3]. Therefore, oversimplifying the kinematic structure is not recommended, as the upper arm is kinematically redundant resulting in high intra-subject variability even for well defined tasks [4].

Almost all existing upper limb exoskeletons use a *hierarchical* kinematic framework (for example, D-H parameters) in estimating upper limb kinematics of the human user. This framework neglects translations of the shoulder articulation and the role of the shoulder grirdle. Even though these methods are simple and useful they have significant limitations like: error propagation into successive levels and error worsening due to bias in the case of joint translations [5], making them unreliable.

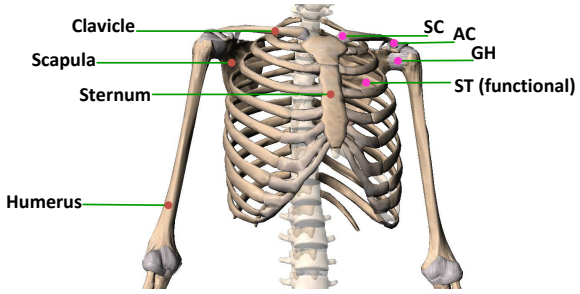

Figure 1: Illustration of human shoulder[3] showing constituent bones and joints: SC-Sternoclavicular, AC-Acromioclavicular, GH-Glenohumeral and ST-Scapulothoracic. Note that, ST is not a physical joint but a functional contact constraint between Scapula and Thoracic cage

Currently, the Euler angles [6] and Globe parametrisation [7] is widely used to report thoracohumeral kinematics. However, these representations introduces geometric singularities in the arm-reachable workspace [8], resulting in ambiguity. Note that the three-angle system is reliable only if independent motions occur in cardinal planes [9]; otherwise, for non-cardinal plane motions, they serve as a crude approximation.

Both of these above mentioned methods assume the shoulder articulation to be a perfect ball and socket joint, which is a non-realistic idealization in our opinion. Because, the humerus rotates and translates simultaneously with respect to the thorax and the validity of this simplifications mainly depends on the joint's congruency [10].

To sum up, existing thoracohumeral kinematic parametrizations are not suitable for high reliability applications. An alternative to hierarchical techniques is the 6-DOF approach. The 6-DOF approach has several advantages like: kinematic decoupling of adjacent segments, and better resolution of non-sagittal plane motions [5]. Further, repeatability of kinematic measurements is improved by decoupling segment kinematics [11].

We propose a 6-DOF approach based on spatial velocities in the form of Hybrid-Twists, motivated by the

*This work was supported by (AAL Call 6) AXO-SUIT project

[1] Computer Vision & Active Perception Lab and BioMEx center, KTH (Royal Institute of Technology), Stockholm, Sweden rkth@kth.se

[2] Department of Electronics, Mathematics and Natural Sciences, University of Gävle, Gävle, Sweden

[3] Anatomical image courtesy Visible Body Skeleton premium

above discussed shortcomings of existing approaches. In this paper, we address the invariance and singularity-free aspects of hybrid twists. We demonstrate that using a minimal set of parameters (see Section III) and minimal markers per segment (see Section III); we can ensure flexibility in marker placement, without compromising repeatability (see Section VII), when using hybrid twists (see Section V and VI).

II. Brief Functional Anatomy

The human shoulder is the joint complex with the highest range of motion (ROM) in the human body due to lack of bony constraints [9]. The dynamic nature of the surrounding musculature and the flexibility of ligaments impart kinematic and dynamic redundancy, facilitating necessary positioning of the human forearm and palm [12].

The musculoskeletal design of the human shoulder is remarkable. It is not a joint in the true sense; rather, it is constituted of individual joints that connect the rigid bones clavicle, humerus and the flat scapula that attaches to the thoracic cavity. The interacting connections between these rigid bones are the following anatomical joints: sternoclavicular (SC), acromioclavicular (AC), glenohumeral (GH), and scapulothoracic (ST) which is a contact constraint between the scapula and thorax, as shown in Fig.1. The kinematics of the shoulder constituent bones are not independent of one another; rather, there is a repeatable and reproducible synchronization, which is well known as "shoulder rhythm". This makes the kinematic parametrisation of the human shoulder more challenging.

III. Preliminaries

To provide a further understanding of the underlying concepts and assumptions, we present the preliminaries associated with the building blocks of our parametrization, i.e., rigid segments.

Definition 3.1: Minimal representation: For a system with n-rigid bodies in space subjected to m constraints, the minimum number of generalized coordinates needed is $6n - m$. For unconstrained spatial motion, six parameters are essential, resulting in 6-DOF models.

Minimal representations are preferred because they result in a lower number of parameters and reduced computational complexity. Such a representation for a humanoid shoulder is presented in [13], in which the authors have used the ISB (International Society of Biomechanics) standard for parametrizing upper limb kinematics [6]. However, the model does not take the joint translations into account.

Definition 3.2: Rigidity: It is the fundamental shape-preserving property that defines a rigid body.

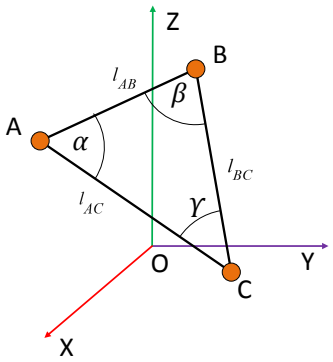

Figure 2: Triad and global reference co-ordinate system. The triad points A, B and C define the lengths and the included angles of the triad.

A rigid transformation is a transformation in which both the Euclidean distance and cross product defined in the rigid body are well preserved [14]; these requirements are canonically embedded in *stiffness constraint*. In reality, the body segments do deform and have inertial effects better known as soft tissue artifacts (STA), which require additional precautions and computations to mitigate.

We define the stiffness constraints mathematically with reference to Fig.2. Let $\mathbf{p_A}$ be the position vector of point A in global co-ordinate frame as shown in Fig. 2. The stiffness condition is six strict constraints concerning the sides and corresponding included angles of the triad given by

$$\|\mathbf{p_i} - \mathbf{p_j}\| = l_{ij}, \tag{1}$$

wherein $i, j = A, B, C$ provided $i \neq j$.

$$\cos\alpha = \frac{(\mathbf{p_B} - \mathbf{p_A}) \cdot (\mathbf{p_C} - \mathbf{p_A})}{l_{AB} l_{CA}}. \tag{2}$$

The relations for β and γ are similar. To track a rigid body, a set of three noncollinear points called a triad is required, and these points are also known as technical markers [15]. Using the triad points, a body-fixed co-ordinate system can be defined.

A. Instantaneous Kinematics: Brief Treatment

Human arm motion is inherently smooth. Therefore, instantaneous kinematic representations are relevant. They are parametrised in terms of infinitesimal rotations and translations, better known as angular and linear velocities.

For any generalized rigid body, as shown in Fig. 3, the instantaneous velocity of a body-fixed point R is given in terms of the velocity $\mathbf{v_A}$ of the origin of body-fixed coordinate system A and angular velocity vector $\boldsymbol{\omega} \in \mathcal{R}^3$ expressed as

$$\mathbf{v_R} = \mathbf{v_A} + \boldsymbol{\omega} \times \mathbf{p_{AR}}. \tag{3}$$

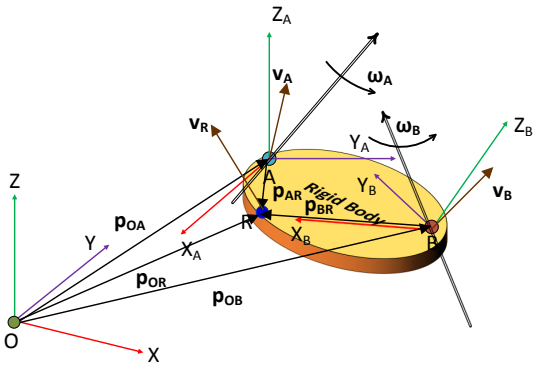

Figure 3: Figure shows a global reference coordinate system and two body-fixed coordinate systems A and B. It can be mathematically proved that the computed angular velocities $\boldsymbol{\omega_A} = \boldsymbol{\omega_B} = \boldsymbol{\omega}$, using the stiffness constraints (1) and generalised velocity in (3) to this figure.

In the case of pure rotation, the solution to (3) is an exponential map.

An important property of the angular velocity is its invariance with respect to the body-fixed axis definition, as illustrated in Fig.3. This property is connected to the uniqueness of Hybrid-twist representation discussed in Section V.

IV. Spatial Kinematic Representation

The spatial kinematic parametrisations can represent simultaneous rotations and translations which is important in the context of thoracohumeral kinematics as discussed in Section I. The twists belong to the spatial kinematic representation and is singularity free. The underlying mathematical structure of twists is the screw, which is defined by Chasles' theorem [16]. Interpretation of this theorem leads to finite twists in the context of position kinematics and twists in the case of instantaneous kinematics.

A. Finite Twist

A finite twist is a screw displacement that is path specific and describes the two locations of the same body or relative displacement between two bodies [16]. It is parametrized by a screw-axis, the angle of rotation about the screw axis and a translation about screw-axis. Finite twists do not form vector subspaces, which means that we cannot combine them or scale them. In [17], finite twists were used to parametrise human thoracohumeral kinematics. However, the pitch of the finite twist cannot be determined uniquely [16].

B. Twist

Twists posses linear properties as, they are parametrized by first-order time derivatives of displacement [16]. Physically, it can be interpreted that the relative motion between two body segments about the joint occurs about several screws of the type 1-system [18]. The line parametrizing the twist represents the set of points on the rigid body with the minimum magnitude of velocities [19].

Depending on the choice of the angular and linear velocities, twist representation comes in different flavors [20]. In this paper, we use the *hybrid-twist* representation, in which angular and linear velocities are referred to the spatial frame.

V. Proposed Approach: Hybrid Twists

Our main motivation to use hybrid twists in our approach is that ambiguity related to the choice of body-fixed frames no longer exists and segmental kinematics is decoupled [20]. Moreover, information in the case of this parametrization is self-contained, i.e., the axis, pitch and the pedal point that describe the hybrid twist can be uniquely derived from a given spatial vector [21], [22].

Fig.4 illustrates how hybrid-twists have been used in parametrizing thoracohumeral kinematics. Mathematically, (3) can be written in the form of spatial vector as,

$$\boldsymbol{\xi} = \begin{bmatrix} \boldsymbol{\omega} \\ \mathbf{v_A} \end{bmatrix} \mathbf{D_A}. \tag{4}$$

A generalised hybrid-twist in terms of instantaneous velocities is defined in (4). The basis vector $\mathbf{D_A}$, that defines hybrid-twists belong to the Plücker basis, for a detailed discussion please refer [22].

Hybrid twists are parametrised using the screw-axis defined by directed line and the pedal point; and the ratio of the translation velocity and angular velocity along the screw-axis, known as the pitch. These concepts are discussed in detail in Section.VI-B.

Hybrid twists have a theoretically guaranteed invariance, which has been derived from first principles in [23]. The strength of property is that the choice of the triad on the rigid body is flexible and is only limited by the measurement system or procedure specifications, unlike other existing 6-DOF representations [10]. In the case of inactivity, when the relative spatial velocity becomes zero, the hybrid-twists have no real meaning or interpretation, which is a limitation.

In the following section, we present the computation of hybrid-twists from the motion capture data and the parameters that determine the hybrid-twist uniquely.

VI. Computation and Measurement

We demonstrate the efficacy hybrid-twists in the scenario of thoracohumeral kinematics, by computing the hybrid-twist parameters and propose a metric to measure the level of agreement between the computed hybrid-twists. The thoracohumeral kinematics is studied by identifying three basic shoulder motions of interest.

A. Computing Angular Velocity Vector, $\boldsymbol{\omega}$

The marker velocities, were computed from the motion capture data (see Section VI-C) using the central difference approximation method. A robust method to compute angular velocities from three non-collinear markers with the approach presented in [19] was used. If $\mathbf{p_i}$ is the position vector of the vertex of the triad and its trajectory velocity is $\dot{\mathbf{p}}_\mathbf{i}$, then the centroid $\mathbf{c}_p$ and its velocity $\mathbf{c}_v$ are given by

$$\mathbf{c}_p = \frac{1}{3}\sum_{i=1}^{3}\mathbf{p_i} \quad , \quad \mathbf{c}_v = \frac{1}{3}\sum_{i=1}^{3}\dot{\mathbf{p}}_\mathbf{i}. \tag{5}$$

An important prerequisite for computing the angular velocity from given data is that it should satisfy the stiffness constraints (1)-(2), embedded as the compatibility condition given in [19]. Let us define two tensors $\mathbf{P}$ and $\dot{\mathbf{P}}$

$$\mathbf{P} = [\mathbf{p_1} - \mathbf{c_p}, \mathbf{p_2} - \mathbf{c_p}, \mathbf{p_3} - \mathbf{c_p}], \tag{6}$$

$$\dot{\mathbf{P}} = [\dot{\mathbf{p}}_\mathbf{1} - \mathbf{c_v}, \dot{\mathbf{p}}_\mathbf{2} - \mathbf{c_v}, \dot{\mathbf{p}}_\mathbf{3} - \mathbf{c_v}]. \tag{7}$$

In order to compute the angular velocity vector $\boldsymbol{\omega}$, we need to compute the tensor $\mathbf{M}$ by,

$$\mathbf{M} = \frac{1}{2}(\mathbf{I}\mathrm{tr}(\mathbf{P}) - \mathbf{P}). \tag{8}$$

Here, $\mathbf{I}$ represents the identity matrix of size 3×3, and $\mathrm{tr}(\cdot)$ is the trace of the matrix. Note that, the $\mathbf{M}$ has guaranteed invertibility if the triad is non-collinear. Now we can compute the angular velocity vector as given below,

$$\boldsymbol{\omega} = \mathbf{M}^{-1}\mathrm{vect}(\dot{\mathbf{P}}), \tag{9}$$

Here, $\mathrm{vect}(\cdot)$ denotes the second-rank tensor to invariant vector operation.

B. Computing the Hybrid-Twist Parameters

The hybrid-twist is defined by the screw-axis and the foot of the perpendicular on the screw-axis, known as pedal point [24], as illustrated in Fig.4. Because the human shoulder lacks bony congruence, its kinematic behavior cannot be captured using a lower kinematic pair assumption; in reality, the joints translate and rotate to some extent.

The screw-axis can be determined by solving (3), for a locus of all points in which the linear velocity occurs in the direction of the angular velocity [24]. The pedal point in the spatial frame is given by

$$\mathbf{r_0} = \frac{\boldsymbol{\omega} \times \mathbf{v_A}}{\|\boldsymbol{\omega}\|^2}. \tag{10}$$

The generalised locus of all the points on the screw axis $\mathbf{x}$, is given by,

$$\mathbf{x} = \mathbf{r_0} + \lambda\boldsymbol{\omega}, \tag{11}$$

where λ is a scalar, of the range $-\infty < \lambda < +\infty$.

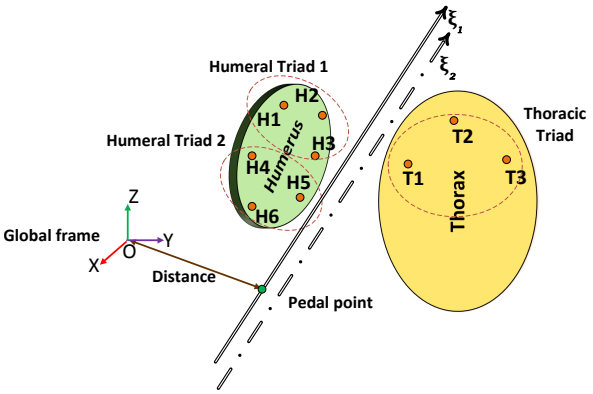

Figure 4: Shows the hybrid twists $\boldsymbol{\xi}_1$ computed from humeral triad 1 (H1-H3) with respect to thoracic triad (T1-T3) and $\boldsymbol{\xi}_2$ is computed from humeral triad 2 (H4-H6) with respect to thoracic triad (T1-T3). Also the concept of the pedal point and its distance is illustrated.

In the event of pure translation, the point $\mathbf{r_0}$ is insignificant because only the direction matters, which is defined by $\mathbf{v_A}$ [22]; however, such a situation seldom arises in a healthy shoulder. It is important to find the pitch h of the screw, which denotes the relationship between the infinitesimal translation and rotation along the screw-axis [22] as

$$h = \frac{\boldsymbol{\omega} \cdot \mathbf{v_A}}{\boldsymbol{\omega} \cdot \boldsymbol{\omega}} = \pm\frac{\|\mathbf{v}_{\mathrm{lin}}\|}{\|\boldsymbol{\omega}\|}. \tag{12}$$

The value of h describes the instantaneous relationship between the angular velocity and translational velocity: zero represents pure rotation, a positive value represents a right-handed screw, and a negative value represents a left-handed screw. While using (10) and (12), one must ensure numerical stability for very small values of $\|\boldsymbol{\omega}\|$.

C. Measurement of Thoracohumeral Kinematics

To compute the relative kinematics, we need to use the relative velocity between the humerus and thorax referred to the spatial frame [22]. Measurements were performed on four healthy male volunteers (given in Tab. I) who did not have any prior history of shoulder pathology. The motion capture was performed using an Optitrak Motive 17 camera system, with a data sampling rate of 120 fps. The trajectories were filtered using a zero-phase Butterworth low-pass filter with a cut-off frequency of 6 Hz.

Each subject was specifically instructed to perform three sets of basic shoulder motions. Subjects performed the motion, at a self-selected pace, in a seated position, starting and ending in the anatomically neutral position, as shown in Fig. 5.

Additionally, each set of activities was performed five times. Specific instructions were given to minimize

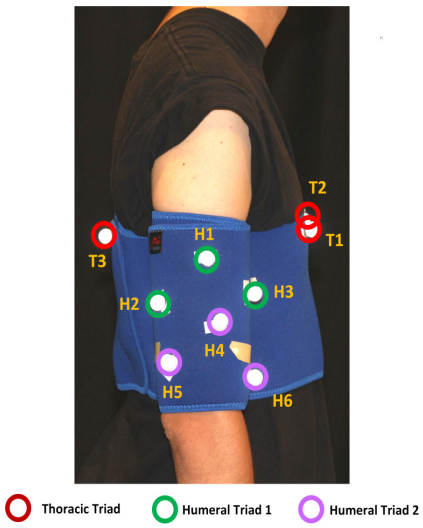

Figure 5: Illustration of 9 passive markers placed on a healthy subject in anatomically neutral position consisting of Thoracic triads (T1-T3), Humeral triad 1 (H1-H3), Humeral triad 2 (H4-H6)

Table I: Details of healthy male subjects involved in the study.

Subject	Age (years)	Weight (kg)	Height (m)	Handedness
1	20	80	1.85	Right
2	28	82	1.75	Right
3	23	70	1.70	Right
4	25	73	1.71	Right

the movements of other body parts as much as possible. To minimize the deformations due to STA, we mounted the markers on braces tightly attached to the thoracic and humeral segments, as shown in Fig. 5. The choice of medio-lateral, superio-inferior and anterior-posterior directions in our measurements; is the positive and negative X, Y and Z-axis of the spatial frame.

A list of three basic shoulder movements were identified, as follows: 1) *Flexion-Extension*: where the relative angles between the humerus with respect to the head decrease and increase in the sagittal plane, respectively; 2) *Abduction-Adduction* (vertical): refers to the motion of the humerus in the coronal plane away and toward the midline of the body; and 3) *Elevation-Depression*: generalized reaching and lowering of the humerus not restricted to cardinal planes. The results to these recorded movements are discussed in detail in Section.VII and the accompanying video submission.

We computed the twist parameters for the basic motions of interest using two humeral marker triads (Humeral triad 1: H1, H2, and H3 and Humeral triad 2: H4, H5, and H6) with respect to the thoracic triads (Thoracic triad: T1, T2, and T3) using Fig. 5. Note that the translational velocity along the screw-axis $\mathbf{v}_{\text{lin}}$ is not uniquely defined until the intensity ω about the screw-axis is known [18].

Table II: RMSD values in m for computed pedal point distance for subjects during three activities: 1) Flexion-Extension, 2) Abduction-Adduction, and 3) Elevation-Depression. Note that, the last row shows the task-specific statistics and last column shows subject-specific statics.

Subject	Task 1	Task 2	Task 3	RMSD Statistics
1	0.112	0.148	0.139	0.133±0.02
2	0.147	0.103	0.088	0.112±0.03
3	0.154	0.087	0.098	0.113±0.03
4	0.120	0.08	0.080	0.093±0.02
Task	0.133±0.02	0.0.104±0.03	0.281±0.02	—

The root mean square deviation (RMSD) of the distance of the pedal point from the origin is computed to understand the extent of agreement between the computed pedal point distances.

VII. Results and Discussion

We present the computed twist parameters and the distance of the pedal point from the origin of the space-fixed coordinate system, pitch and the RMSD for the computed distances. For sake of clarity, readers are encouraged to go through the accompanying video content as well. Note that, the results are person-specific in nature and depends on the nature of movement. So, it is expected that the shape of computed pitch and pedal-point distances would in turn depend on the activity being studied.

In the case of ideal rigid behavior, the computed pitches and the distance of the pedal point must overlap. However, in the case of human movement, there are inertial effects of soft tissue, which create relative movements between the humeral triads, leading to some mismatch. This level of mismatch between computed pedal point distances is expressed in terms of RMSD values is presented in Tab.II. As can be seen, the minimal mean RMSD value occurs during Abduction-Adduction task when the STA is also mininmum, supporting our claim that the representation is invariant of marker placement. Note that, ideally RMSD values need to be as small as possible for high-reliability applications.

A. *Flexion-Extension*

As shown in Fig.6, the flexion phase starts with an external rotation and translation toward the anterio-superior direction, resulting in a positive pitch. Correspondingly, the extension phase ends with an internal rotation and translation in the anterio-inferior direction, resulting in a negative pitch.

B. *Abduction-Adduction (vertical)*

With reference to Fig.7, the initial phase of abduction is marked by a nearly pure rotation. To obtain maximal abduction, there is external rotation accompanied by

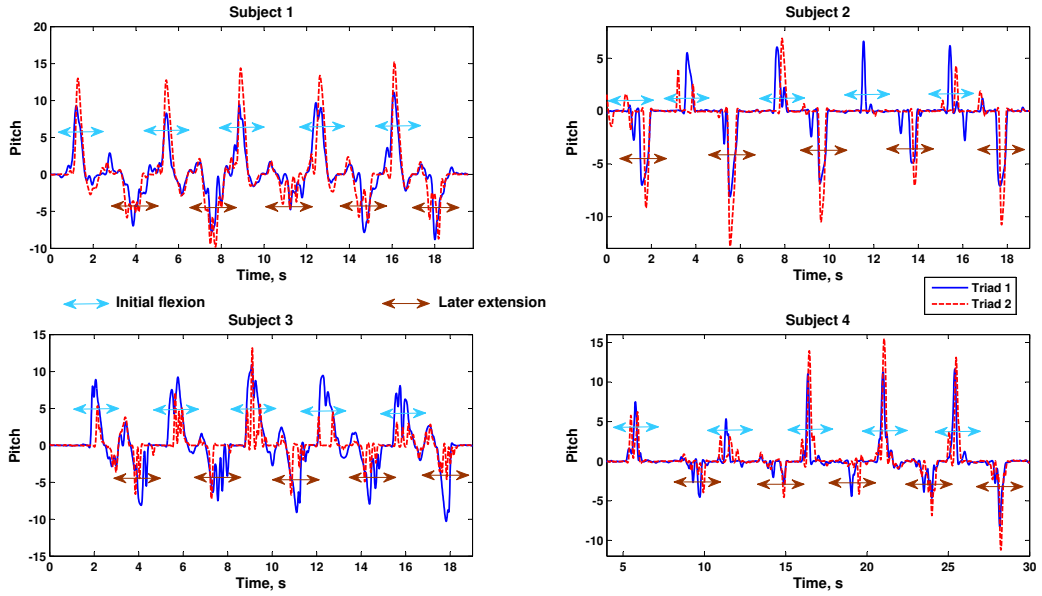

Figure 6: Plots present the computed pitch for four subjects during Flexion-Extension task.

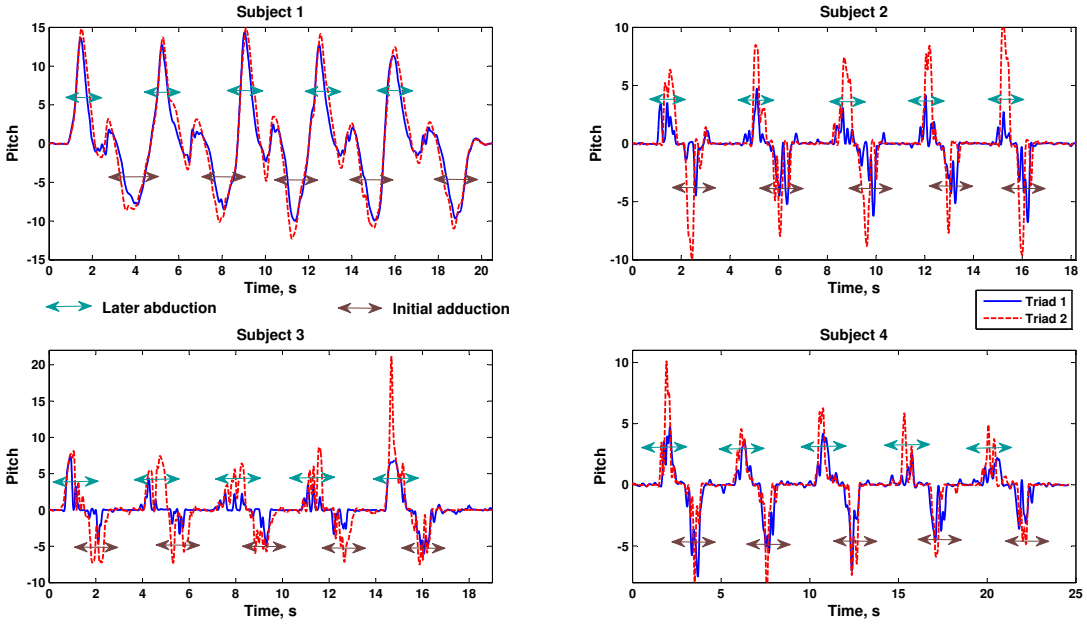

Figure 7: Plots illustrate the computed pitch values for four subjects during an Abduction-Adduction task.

translation in the latero-superior direction, resulting in a positive pitch. The plot of the distance of the pedal point substantiates the nearly pure rotation of the humerus, in which the distance is nearly constant as shown in Fig.8. The reverse occurs in the case of humeral adduction. This consistent pattern may be due to the maximum congruency of humeral head on the glenoid socket.

C. Elevation-Depression

In contrast to the previous two activities, the external rotation of the humerus occurs throughout the elevation phase and the depression is characterised by internal rotation about the humerus, accompanied by translation in the anterio-superior and anterio-inferior directions, resulting in positive and negative pitches; see Fig.9 .

Thus, the study clearly demonstrates that hybrid-twists is free of singularities and that the parametrization can be used to differentiate various thoracohumeral movements reliably. We can see a consistent pattern in our results, which is activity-specific and the observed features are generalisable across different subjects. Note that the ringing peak-like phenomenon in the pitch curves, is due to the inertial effects of the STA that cannot be mitigated by the brace supports. We believe that numerical preprocessing of the marker data could improve the practical use of hybrid-twists. Thus, hybrid-twists does hold a potential to improve the reliability of estimated thoracohumeral kinematics, for high-reliability human-machine applications.

VIII. Conclusions

We have successfully demonstrated that the humeral rotations can be robustly parametrized using the hybrid twists despite the measurement limitations because they are free of geometric singularities. Additionally, we have also successfully verified that the parametrization is invariant of the marker placement, thereby providing additional flexibility. Thus, we were able to parametrize thoracohumeral kinematics with a minimal set of parameters, using minimal markers per segment in the context of instantaneous kinematics with high repeatability and reproducibility. Note that preprocessing steps aimed at minimising inertial effects of STA can improve the repeatability. Parametrising and interpreting complex shoulder motions using hybrid twists is an interesting problem we would like to explore further.

Acknowledgements

Authors would like to acknowledge the subjects who have volunteered for the study.

References

[1] Y. Mao *et al.*, "Human Movement Training With a Cable Driven ARm EXoskeleton (CAREX)," *IEEE Trans. Neural Syst. Rehabil. Eng.*, vol. 23, no. 1, pp. 84–92, jan 2015.

[2] N. Jarrassé *et al.*, "Robotic Exoskeletons: A Perspective for the Rehabilitation of Arm Coordination in Stroke Patients," *Front. Hum. Neurosci.*, vol. 8, no. December, pp. 1–13, 2014.

[3] J. Pons, "Rehabilitation exoskeletal robotics," *IEEE Eng. Med. Biol. Mag.*, vol. 29, no. 3, pp. 57–63, 2010.

[4] C. J. VanAndel *et al.*, "Complete 3D kinematics of upper extremity functional tasks." *Gait Posture*, vol. 27, no. 1, pp. 120–7, jan 2008.

[5] A. Schmitz *et al.*, "Comparison of hierarchical and six degrees-of-freedom marker sets in analyzing gait kinematics," *Comput. Methods Biomech. Biomed. Engin.*, vol. 19, no. 2, pp. 199–207, 2016.

[6] G. Wu *et al.*, "ISB recommendation on definitions of joint coordinate systems of various joints for the reporting of human joint motion Part II: shoulder, elbow, wrist and hand," *J. Biomech.*, vol. 38, no. 5, pp. 981–992, 2005.

[7] M. L. Pearl *et al.*, "A system for describing positions of the humerus relative to the thorax and its use in the presentation of several functionally important arm positions," *J. Shoulder Elb. Surg.*, vol. 1, no. 2, pp. 113–118, 1992.

[8] T. Masuda *et al.*, "A proposal for a new definition of the axial rotation angle of the shoulder joint." *J. Electromyogr. Kinesiol.*, vol. 18, no. 1, pp. 154–9, feb 2008.

[9] D. Haering *et al.*, "Measurement and description of three-dimensional shoulder range of motion with degrees of freedom interactions," *J. Biomech. Eng.*, vol. 136, no. 8, pp. 1–6, 2014.

[10] E. Cattrysse *et al.*, "Intra-articular kinematics of the upper limb joints: a six degrees of freedom study of coupled motions." *Ergonomics*, vol. 48, no. 11-14, pp. 1657–1671, 2005.

[11] A. Cappozzo *et al.*, "Position and orientation in space of bones during movement : anatomical frame definition and determination," *Clin. Biomech.*, vol. 10, no. 4, pp. 171–178, 1995.

[12] W. T. Dempster, "Mechanisms of Shoulder Movement," *Arch. Phys. Med. Rehabil.*, vol. 46, pp. 49–70, jan 1965.

[13] D. Ingram *et al.*, "A minimal set of coordinates for describing humanoid shoulder motion," in *Intelligent Robots and Systems (IROS), 2013 IEEE/RSJ International Conference on*, Nov 2013, pp. 5537–5544.

[14] R. M. Murray *et al.*, *A Mathematical Introduction to Robotic Manipulation*. CRC press, 1994.

[15] A. Cappozzo *et al.*, "Human movement analysis using stereophotogrammetry. Part 1: theoretical background." *Gait Posture*, vol. 21, no. 2, pp. 186–196, 2005.

[16] J. K. Davidson and K. H. Hunt, *Robots and Screw Theory: Applications of Kinematics and Statics to Robotics*. New York, USA: Oxford University press, 2004.

[17] A. E. Engín, "On the biomechanics of the shoulder complex." *J. Biomech.*, vol. 13, pp. 575–590, 1980.

[18] L.-W. Tsai, *Robot Analysis and Design: The Mechanics of Serial and Parallel Manipulators*. John Wiley and Sons, 1999.

[19] J. Angeles, *Fundamentals of Robotic Mechanical Systems : Theory , Methods , and Algorithms.*, 2nd ed., 2003.

[20] A. Müller, "Higher derivatives of the kinematic mapping and some applications," *Mech. Mach. Theory*, vol. 76, pp. 70–85, 2014.

[21] H. Bruyninckx, *Robot Kinematics and Dynamics*, Leuven, Belgium, 2010.

[22] R. Featherstone, *Rigid Body Dynamics Algorithms*. Springer US, 2008.

[23] J. Awrejcewicz, *Classical Mechanics: Kinematics and Statics*, ser. Advances in Mechanics and Mathematics. New York, NY: Springer New York, 2012.

[24] H. W. Guggenheimer, "Formulas of Linear Geometry," *Coll. Math. J.*, vol. 27, no. 1, pp. 24–32, 1996.

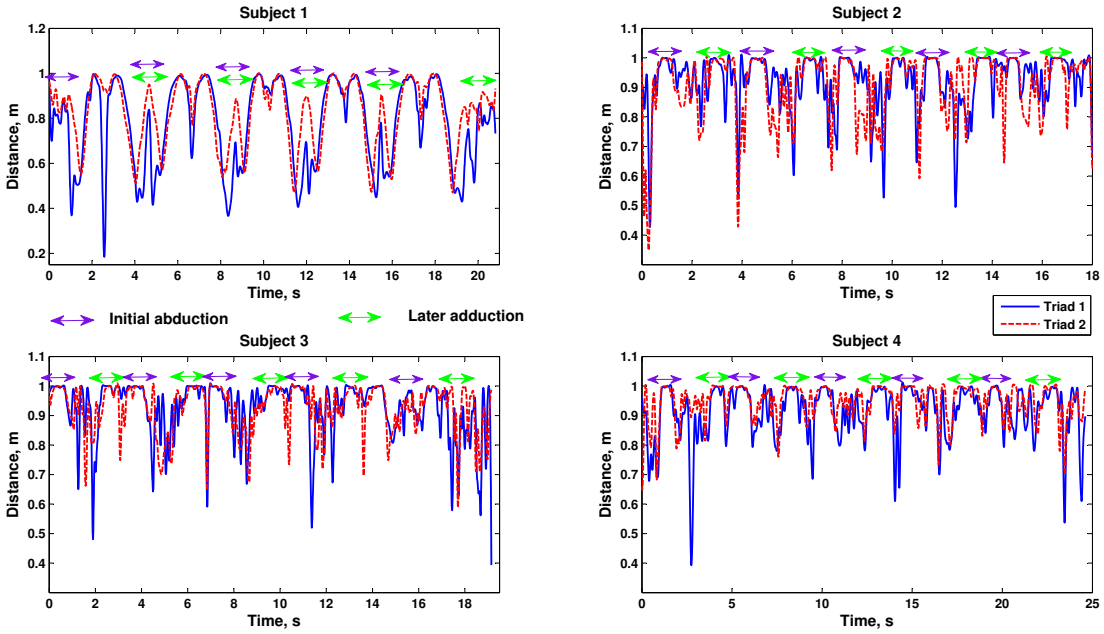

Figure 8: Plots show distance of the pedal point for four subjects during Abduction-Adduction task.

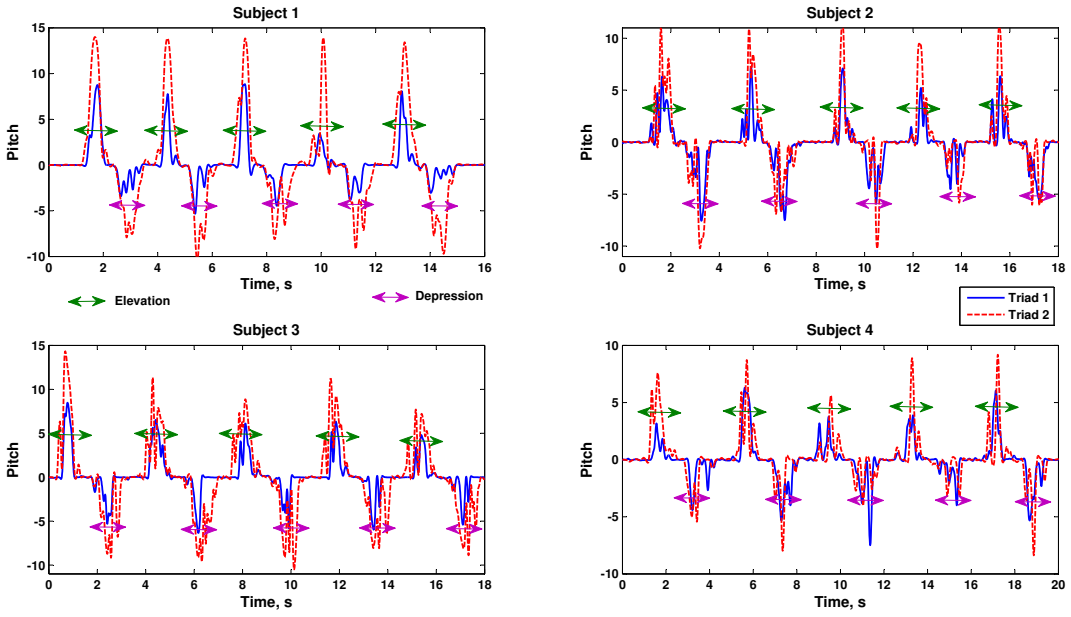

Figure 9: Plots show the computed pitch values for four subjects during Elevation-Depression task.